Energy 188 (2019) 116047

Contents lists available at ScienceDirect

Energy

journal homepage: www.elsevier.com/locate/energy

Review

A novel analytical solution for the calculation of temperature in supercapacitors operating at constant power

Joaquín F. Pedrayes*, Manuel G. Melero, Joaquín G. Norniella, José M. Cano, Manés F. Cabanas, Gonzalo A. Orcajo, Carlos H. Rojas

Departamento de Ingeniería Eléctrica, Electrónica, de Computadores y Sistemas, Universidad de Oviedo, Spain

ARTICLE INFO

Article history:
Received 16 February 2019
Received in revised form
29 July 2019
Accepted 31 August 2019
Available online 5 September 2019

Index Terms:
Constant power operation
Supercapacitors
Thermal modelling

ABSTRACT

Temperature evolution in supercapacitors (SCs) when they are charged or discharged at a constant current is a well-known process. However, it does not exist any mathematical equation for the calculation of the instantaneous temperature of the SC when it is charged or discharged at constant power. In this work, a new mathematical formulation is presented, which allows for the analytical calculation of temperature as a function of time (or alternatively, as a function of the current or the internal or the external voltage), considering the electrical and thermal properties provided by the manufacturer of the SC or obtained through laboratory tests. Highly accurate equations for the calculation of instantaneous current, power losses and other significant variables are also obtained. The validity of the proposal is demonstrated by comparing the results obtained with the new method with those yielded from the classical iterative, numerical resolution of the differential equations. The high accuracy of the proposed approach makes it useful to be used in the task of sizing the cooling systems of SC applications.

Contents

1. Introduction

Recent advances in manufacturing have made supercapacitors (SCs) a feasible alternative to other electrical energy storage devices [1]. Their main advantage, in comparison to batteries, is their capability to handle high charge and discharge currents thanks to their low internal resistance and large specific power [2]. Moreover, the life cycle of SCs is several orders of magnitude higher than the one of batteries, even for the case of battery cells manufactured with the most resistant chemical compositions [3].

Hybrid sets, where SCs and batteries work together, are becoming a prominent solution for applications requiring energy storage [4–9]. In these cases, SCs are used to provide or absorb peaks of power which, despite their low internal resistance, can lead to a remarkable internal heating. Thus, the temperature

* Corresponding author.
E-mail address: pedrayesjoaquin@uniovi.es (J.F. Pedrayes).

https://doi.org/10.1016/j.energy.2019.116047

reached by the SC cells in a particular application should be taken into account during the design stage, as this fact determines the cooling system to be used and the electrical behaviour of the device.

The values of the internal parameters of a SC depend on temperature, although their variability is different according to the temperature span within which they are used. The usual range of temperature that ensures cell integrity and durability goes from 20 °C to 65 °C. Within this range, the variation of cell parameters can be considered negligible. For this reason, internal resistance and capacity will be considered as constant values in this study, thus assuming that the operation of the SC takes place within normal operational limits. It is interesting to highlight that, beyond this temperature span, the electrical values of these parameters strongly change and the performance of the device deteriorates to the point that internal degradation may appear. Specifically, below 0 °C the viscosity of the electrolyte increases yielding a drastic reduction in electrical conductivity. Moreover, the solubility of conductive salts decreases, and hence the internal resistance rises up. On the other hand, if the temperature is too high, Helmholtz layer enlarges over the surface of the electrolyte producing a reduction in the capacity of the cell of up to 2% of its rated value [10]. In addition to the effects of the temperature over the electrical parameters of SCs, operation out of the range −40 °C to 65 °C leads to the degradation of the electrolyte. The service life of the SC mostly depends on the operation voltage range and mean temperature [11–17]. Thus, a proper estimation and control of the temperature in SC banks is critical to get a successful operation and a long lifespan of the system [18]. The calculation of the temperature of the SC is essential to design the cooling system, to size the cells and their capacity for facing a specific power profile, and to foresee their service life.

Therefore, the design stage should foresee the temperature that the SC can reach when subjected to a succession of charge/discharge processes. Some studies have been conducted to analyse the thermal behaviour of SCs operating at constant charge or discharge currents [19,20]. However, no equation exists to describe the evolution of the instantaneous temperature of the cell when it operates at constant charge or discharge power. Such kind of equation can highly improve the process of selecting the optimum cooling system for a particular application using SCs operated at constant power.

In Ref. [21], a smartly simplified approach to constant power operation is presented. In this study, the analytical solution for the temperature as a function of time turns out to be an exponential or single pole response, which is the same case arising at constant current operation. Although the study is comprehensively presented and cleverly simplified, the results are not completely able to track the instantaneous temperature of the SC in an actual application where the SCs banks are operated at constant power.

To carry out the present study, the thermal model of the SC described by Grbovic [22], as well as the characterization of the behaviour of the SC operated at a constant power developed by Miller [21], are taking as accepted basis. Following the methodology of previous research studies [23–28], the assessment of the accuracy of the proposed formulation is carried out by comparing its results with those yielded by the numerical solution, free of any approximation, of the differential equation that models the process.

This work is organized according to the following structure. In section 2, the evolution of the current, power losses and energy losses, when the SC operates at a constant power, is presented. Both the classical formulation and the new equations are derived in this section. Section 3 shows a case study in which the exact value of intermediate variables of a cell providing a constant power, needed in the process of temperature calculation, are compared with those estimations attained from the classical and new equations in order to assess the accuracy of the proposal. Section 4 introduces a new expression for the calculation of the instantaneous temperature of the cell as function of time, internal and external voltages and current. Section 5 shows two case studies in which the accuracy of the estimation of the temperature of the cell through the new mathematical modelling is assessed and demonstrated. Finally, section 6 summarizes the most important results of this study.

2. Analysis of SCs operated at constant power

The model of a SC bank discharged at a constant power value, P, is shown in Fig. 1. This model is characterized through the equivalent resistance, R, capacitance, C, internal voltage, u, and external voltage, u_{C0}.

In the following and for the sake of simplicity, time functions in the form $f(t)$ are represented as f and their derivatives, $\frac{df(t)}{dt}$, as f'. Capital letters are used to refer to constants. According to the said model

$$P + R \cdot i^2 = u \cdot i. \tag{1}$$

According to Kirchhoff's Voltage Law, the internal voltage of the SC bank can be expressed as

$$u = u_{co} + R \cdot i, \tag{2}$$

where i stands for the current flowing out of the cell. Considering the state equation of the capacitance,

$$u' = -\frac{i}{C}. \tag{3}$$

By deriving (1) and combining it with (3), the following differential equation is obtained,

$$0 = -i^3 + C \cdot \left(P - R \cdot i^2\right) \cdot i'. \tag{4}$$

The mathematical statement in (4) comprises a separated variables differential equation which allows the calculation of time as a function of current. However (4), does not allow a straightforward calculation of current as a function of time. In order to enable obtaining the current, it can be assumed that losses in the internal resistance, R, are negligible as compared to the total power, i.e.

$$P \gg R \cdot i^2 \overset{yields}{\rightarrow} R \cdot i^2 \approx 0. \tag{5}$$

Under the assumption in (4), (5) can be rewritten as

$$i^3 \approx C \cdot P \cdot i'. \tag{6}$$

Equation (6) can be solved by considering, as an initial condition, that the internal and external voltages of the cell are equal at time

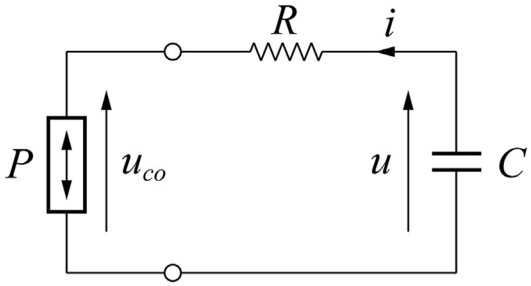

Fig. 1. Discharge of a SC at constant power.

zero. Let us use u_o to stand for this initial voltage value. Thus, current can be expressed as a function of time as

$$i \approx P \cdot \sqrt{\frac{C}{C \Delta u_0^2 - 2 \cdot P \cdot t}}. \tag{7}$$

Once current is known, losses caused by the internal resistance, R, can be directly calculated as

$$P_{losses} = R \cdot i^2 \approx \frac{C \cdot R \cdot P^2}{C \cdot u_0^2 - 2 \cdot P \cdot t}. \tag{8}$$

Therefore, the energy transformed into heat can be calculated as

$$W_{losses} = \int_0^t P_{losses} \cdot dt \approx -\frac{R \cdot P \cdot C}{2} \cdot \ln\left(1 - \frac{2 \cdot P \cdot t}{C_o \cdot u_0^2}\right). \tag{9}$$

The above equations yield accurate results at moderate current levels. However, when the depth of discharge (DoD) of the cell is large or at high power levels the error increases, since the aforementioned assumption stated in (5) is no longer valid, i.e. power losses cannot be neglected at those operating conditions. In order to improve accuracy in the calculation of current, an alternative method of analysis is introduced in this work. This new method requires an earlier calculation of the internal voltage, u, as a function of time. Thus, by combining (1) and (3), the following relation is attained

$$R \cdot C^2 \cdot u'^2 + C \cdot u \cdot u' + P = 0. \tag{10}$$

If (10) is divided by $R \cdot C^2$, then

$$u'^2 + \frac{u}{R \cdot C} \cdot u' + \frac{P}{R \cdot C^2} = 0, \tag{11}$$

where $P > 0$ for a discharge and $P < 0$ for a charge. Solving (11) for $\boldsymbol{u'}$ yields

$$u' = \frac{-u}{2 \cdot R \cdot C} + \frac{\sqrt{u^2 - 4 \cdot P \cdot R}}{2 \cdot R \cdot C}. \tag{12}$$

Thus, the time, t, needed by the internal voltage to reach each current value, u, from the initial one, u_0, can be obtain from (12) as

$$t = \frac{C}{4 \cdot P} \cdot \left[u_0^2 + u_0 \cdot \sqrt{u_0^2 - 4 \cdot \mathrm{P} \cdot \mathrm{R}} - u^2 - u \cdot \sqrt{u^2 - 4 \cdot P \cdot R} - 4 \cdot P \cdot R \cdot ln\left(\frac{u_0 + \sqrt{u_0^2 - 4 \cdot P \cdot R}}{u + \sqrt{u^2 - 4 \cdot P \cdot R}}\right)\right]. \tag{13}$$

Let us define the function $h(u_0)$ as follows

$$h(u_0) = u_0^2 + u_0 \cdot \sqrt{u_0^2 - 4 \cdot P \cdot R}. \tag{14}$$

Equation (13) is formed by five addends. The fifth one is affected by a logarithmic fraction that makes this term negligible when compared to the values of the other four. Taking this fact into account, the following equation can be obtained

$$u^2 + u \cdot \sqrt{u^2 - 4 \cdot P \cdot R} \approx h(u_0) - \frac{4 \cdot P \cdot t}{C}. \tag{15}$$

A change of variable is now needed to calculate the SC internal voltage, u. The new variable, z, is defined as

$$z = -u + \sqrt{u^2 - 4 \cdot P \cdot R}. \tag{16}$$

Operating on (16), two terms appearing in (15) can now be expressed as a function of the newly defined intermediate variable, z,

$$u = \frac{-z}{2} - \frac{2 \cdot R \cdot P}{z}, \tag{17}$$

$$\sqrt{u^2 - 4 \cdot P \cdot R} = \frac{z}{2} - \frac{2 \cdot R \cdot P}{z}. \tag{18}$$

Replacing (17) and (18) in (15) leads to

$$z = \pm 2 \cdot R \cdot P \sqrt{\frac{2}{f(u_0) - \frac{4 \cdot P \cdot t}{C}}}, \tag{19}$$

where $f(u_0)$ is defined

$$f(u_0) = h(u_0) - 2 \cdot R \cdot P. \tag{20}$$

Since the internal voltage, u, is always positive in real SC applications, only the solution preceded by the minus sign in (19) must be considered. Thus, by replacing z in (17) the internal voltage can be expressed as a function of time as

$$u \approx \frac{R \cdot P}{g} + g, \tag{21}$$

where g is defined as

$$g = \sqrt{\frac{1}{2} \cdot f(u_0) - \frac{2 \cdot P \cdot t}{C}}. \tag{22}$$

Once u is known, i can also be calculated. In order to do so, noticed that the derivative of the internal voltage can be obtained from (21) as

$$u' = \frac{du}{dg} \cdot \frac{dg}{dt} = \frac{-R \cdot P \cdot g'}{g^2} + g'. \tag{23}$$

Furthermore, the derivative of the newly defined function g, as expressed in (22), can be obtained as

$$g' = \frac{dg}{dt} = \frac{-P}{C \cdot \sqrt{\frac{1}{2} \cdot f(u_0) - \frac{2 \cdot P \cdot t}{C}}} = \frac{-P}{C \cdot g}. \tag{24}$$

Using the state equation of the capacitance (3), together with (23) and (24), i can be obtained as a function of g as

$$i \approx \frac{P}{g} \cdot \left[1 - \frac{R \cdot P}{g^2}\right]. \tag{25}$$

Practical SC values fulfill the following condition

$$1 \gg \frac{R \cdot P}{g^2}. \tag{26}$$

Thus, the current, i, can be approximately expressed as

$$i \approx \frac{P}{g}. \tag{27}$$

By replacing the value of g in (27) as defined in (22), a new expression for the current is finally obtained,

$$i \approx P \cdot \sqrt{\frac{C}{\frac{C}{2} \cdot f(u_0) - 2 \cdot P \cdot t}}. \tag{28}$$

This new equation is apparently similar to the classical formulation presented in (7). Notice that the term u_0^2 used in (7) is replaced in (28) by $0.5 \cdot f(u_0)$. However, in spite of this resemblance, the results yielded by (28) present an extremely low error level as it is demonstrated in section 3.

From (27), the power losses in the SC cell can be easily assessed as

$$P_{losses} = R \cdot i^2 \approx \frac{R \cdot P^2}{g^2}. \tag{29}$$

By definition, power losses are the derivative of energy losses with respect to time. Thus, they can be expressed as

$$P_{losses} = W_{losses}{}' = \frac{dW_{losses}}{dg} \cdot g'. \tag{30}$$

If the derivative of function g, as given in (24), is replaced in (30), the integration of the resulting expression leads to

$$W_{losses} \approx R \cdot C \cdot P \cdot Ln\left(\frac{g_0}{g}\right), \tag{31}$$

where g_0 stands for the value of function g at time zero. Finally, by replacing the values of g and g_0 in (31), an improved equation for the calculation of energy losses is attained,

$$W_{losses} \approx -\frac{R \cdot C \cdot P}{2} \cdot \mathrm{Ln}\left(1 - \frac{4 \cdot P \cdot t}{C \cdot f(u_0)}\right). \tag{32}$$

3. Assessment of proposed equations

To assess the accuracy of the proposed analytical equations (28) and (32), their results are compared to those yielded when solving differential equation (4) by using numerical methods, which provide the exact solution, or by utilizing the classical approximations given by equations (7) and (9). This comparison proves the errors arising from the application of the proposed analytical approach to be lower than those occurred when using the classical approximations. Since the proposed analytical equations are much simpler than the numerical-method-based ones, the computational effort is reduced when the former are applied.

A case study comprising the discharge of a SCs bank is simulated according to the parameters shown in Table 1.

Fig. 2 shows the evolution of the discharge current obtained by using numerical methods (blue plot, exact solution), the classical approximation (red plot), and the proposed analytical equation (28), (green plot). Only the last 20 s of the discharge have been plotted to better observe the differences among the three approaches.

Fig. 3 shows the percentage error occurred in calculating the discharge current when using the classical or the proposed approximations,

Table 1
Parameters of the SCs bank.

C (F)	R (mΩ)	u_0 (V)	P(W)	$t_{discharge}$ (s)
150	40	135	3000	140

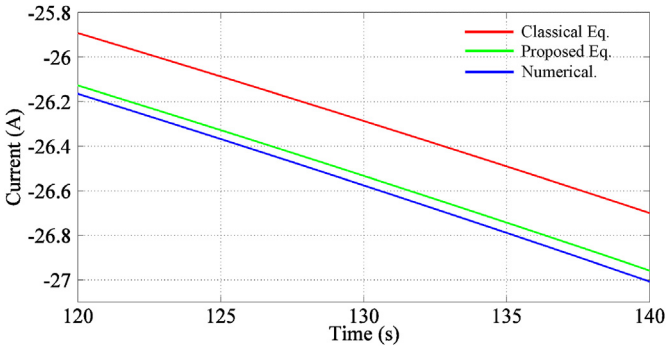

Fig. 2. SCs bank discharge current when using numerical methods (blue plot), the classical approximation (red plot), and the proposed analytical equation (green plot). (For interpretation of the references to colour in this figure legend, the reader is referred to the Web version of this article.)

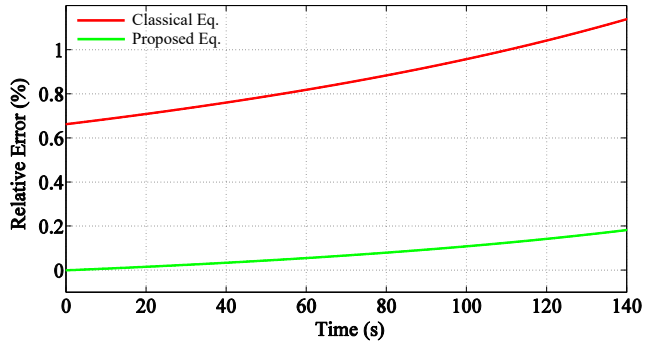

Fig. 3. Discharge current error when using the classical approximation (red plot), and the proposed analytical equation (green plot). (For interpretation of the references to colour in this figure legend, the reader is referred to the Web version of this article.)

$$Error(\%) = \frac{|i_{exact} - i_{estimated}|}{i_{exact}} \cdot 100. \tag{33}$$

As shown in Figs. 2 and 3, both the absolute value of the current and the error increase as the discharge progresses; however, the error arisen from using the proposed approximation is always lower than that occurred when utilizing the classical one. The initial error when using the proposed equation is null because $u = u_0$ at $t = 0$ s and, therefore, the Napierian logarithm in (13) equals 0. Fig. 4

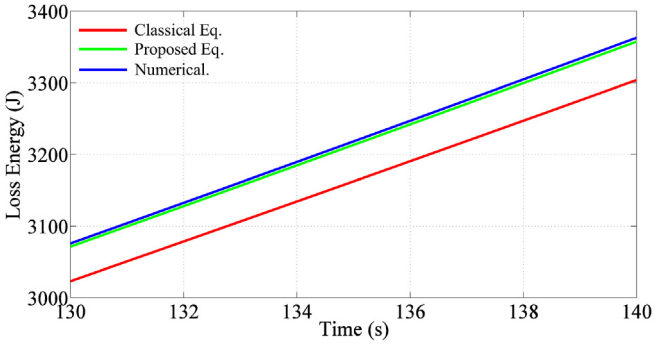

Fig. 4. Energy dissipated during the discharge by using numerical methods (blue plot), the classical approximation (red plot), and the proposed analytical equation (green plot). (For interpretation of the references to colour in this figure legend, the reader is referred to the Web version of this article.)

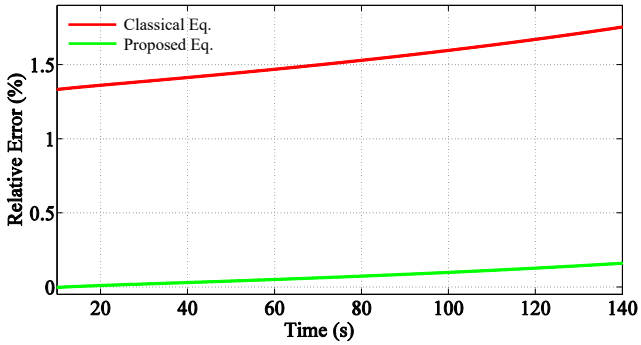

Fig. 5. Dissipated energy error when using the classical approximation (red plot) and the proposed analytical equation (green plot). (For interpretation of the references to colour in this figure legend, the reader is referred to the Web version of this article.)

shows the evolution of the energy dissipated during the discharge process. Only the last 10 s of the discharge have been plotted to better observe the differences among the three approaches. Fig. 5 shows the corresponding error arisen from using the classical or the proposed approximation. As can be seen in both figures, the proposed analytical equation, (32), is more accurate than the classical one.

Once the equations proposed to calculate the discharge current and the dissipated energy have been obtained and validated, the evolution of the temperature of a SCs bank as a function of time, the current, and the internal and external voltages is obtained for a constant-power charge/discharge process.

4. Thermal model

The thermal model of the SC is based on the classical analogy with the electric circuit in Fig. 6, where P_{losses} represents the power losses at the internal resistance of the cell, P_{amb} stands for the heat power losses, T_{amb} is the ambient temperature, T is the temperature of the cell, $P_{internal}$ is the rate of change of stored heat energy in the SC, and R_{TH} and C_{TH} are, respectively, the thermal resistance and capacitance of the cell. Both R_{TH} and C_{TH} are usually provided by the manufacturer or can be calculated by conducting simple experimental tests.

The differential equation that determines the thermal behaviour of the cell is

$$P_{losses} = C_{TH}\cdot\theta' + \frac{\theta}{R_{TH}}, \tag{34}$$

θ being the thermal jump between the temperature of the cell and the ambient temperature,

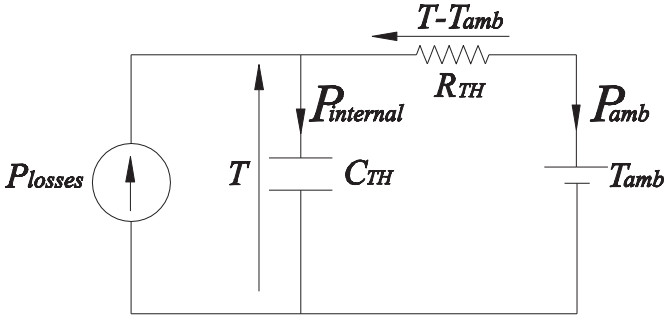

Fig. 6. Thermal model.

$$\theta = T - T_{amb}. \tag{35}$$

Equation (34) can be expressed as a function of time as an independent variable by using equation (8) or equations (22) and (29), the utilization of (22) and (29) being more accurate. However, the resulting differential equation cannot be solved via analytical methods; therefore, a change of variables is needed, which can be obtained through variable g by relating equations (29) and (34),

$$\frac{R\cdot P^2}{g^2} = C_{TH}\cdot\frac{d\theta}{dg}\cdot g' + \frac{\theta}{R_{TH}}. \tag{36}$$

The derivative of θ with respect to g can be calculated by relating (24) and (36),

$$\frac{d\theta}{dg} = \left[\frac{C}{C_{TH}\cdot R_{TH}\cdot P}\right]\cdot g\cdot\theta - \left[\frac{R\cdot C\cdot P}{C_{TH}}\right]\cdot\frac{1}{g}. \tag{37}$$

By defining constants a and b,

$$a = \frac{C}{C_{TH}\cdot R_{TH}\cdot P}, \tag{38}$$

$$b = -\frac{R\cdot C\cdot P}{C_{TH}}, \tag{39}$$

equation (37) can be expressed in a much simpler way,

$$\frac{d\theta}{dg} = a\cdot g\cdot\theta + b\cdot\frac{1}{g}. \tag{40}$$

The general solution of (40) can be obtained as

$$\theta(g) = k\cdot\exp\left(\frac{a\cdot g^2}{2}\right) + \frac{1}{2}\cdot b\cdot\exp\left(\frac{a\cdot g^2}{2}\right)\cdot Ei\left(-\frac{a\cdot g^2}{2}\right), \tag{41}$$

where k is the constant of integration and Ei is the so-called exponential integral function,

$$Ei(x) = \begin{cases} \int_{-\infty}^{x}\frac{e^v}{v}\cdot dv & x<0 \\ \lim_{\varepsilon\to 0}\left(\int_{-\infty}^{-\varepsilon}\frac{e^v}{v}\cdot dv + \int_{\varepsilon}^{x}\frac{e^v}{v}\cdot dv\right) & x>0. \end{cases} \tag{42}$$

The constant of integration can be obtained from (41) as

$$k = \theta_0\cdot\exp\left(-\frac{a\cdot g_0^2}{2}\right) - \frac{1}{2}\cdot b\cdot Ei\left(-\frac{a\cdot g_0^2}{2}\right). \tag{43}$$

where $\theta_0 = T_0 - T_{amb}$, T_0 being the temperature of the cell in t = 0 and assumed to be known. By combining (41) and (43), the value of θ as a function of g can be calculated as

$$\theta(g) = \theta_0\cdot exp\left(\frac{a\cdot(g^2-g_0^2)}{2}\right) + \frac{b}{2}\cdot exp\left(\frac{a\cdot g^2}{2}\right)\cdot\left(Ei\left(-\frac{a\cdot g^2}{2}\right) - Ei\left(-\frac{a\cdot g_0^2}{2}\right)\right). \tag{44}$$

The temperature of the cell as a function of g can be obtained by relating (35) and (44),

$$T(g) = T_{amb} + (T_0 - T_{amb}) \cdot exp\left(\frac{a \cdot (g^2 - g_0^2)}{2}\right) + \frac{b}{2} \cdot exp\left(\frac{a \cdot g^2}{2}\right) \cdot \left(Ei\left(-\frac{a \cdot g^2}{2}\right) - Ei\left(-\frac{a \cdot g_0^2}{2}\right)\right). \quad (45)$$

Equation (45) is valid within the typical SC operation range from 0 °C to 65 °C because the electric parameters of the cell, R and C, barely change over that range.

By relating (22) and (45), the temperature of the cell as a function of time can be obtained as

$$T(t) = T_{amb} + \left(k_c + k_b \cdot Ei\left(\frac{t}{\tau_{TH}} - k_a\right)\right) \cdot exp\left(-\frac{t}{\tau_{TH}}\right), \quad (46)$$

where τ_{th} is the thermal constant of the cell, which can be obtained as the product of R_{TH} and C_{TH}. Constants k_a, k_b and k_c can be calculated as

$$k_a = \frac{a \cdot g_0^2}{2} = \frac{C \cdot f(u_0)}{4 \cdot C_{TH} \cdot R_{TH} \cdot P} = \frac{1}{4} \cdot a \cdot f(u_0), \quad (47)$$

$$k_b = \frac{1}{2} \cdot b \cdot \exp(k_a), \quad (48)$$

$$k_c = T_0 - T_{amb} - k_b \cdot Ei(-k_a). \quad (49)$$

Notice that the evolution of the temperature when the SC operates at constant current is similar to that given by (46) without the exponential integral function. Therefore, typical constant-current single-pole temperature responses are not valid to analyse the behaviour of an actual SCs bank, whose usual operation is based on cyclic constant-power charge and discharge processes.

From (45), not only can the temperature be expressed as a function of time, as seen in (46), but also as a function of the internal voltage, the external voltage and the current. From (21), g^2 can be calculated as function of the internal voltage, u,

$$g^2(u) = \frac{u}{2} \cdot \left(u + \sqrt{u^2 - 4 \cdot P \cdot R}\right) - R \cdot P. \quad (50)$$

By combining (45) and (50), the temperature as a function of the internal voltage is obtained,

$$T(u) = T_{amb} + (T_0 - T_{amb}) \cdot exp(m(u) - m_0) - \frac{R \cdot C \cdot P}{2 \cdot C_{TH}} \cdot exp(m(u)) \cdot (Ei(-m(u)) - Ei(-m_0)), \quad (51)$$

$m(u)$ and m_0 depending on u and u_0, respectively,

$$m(u) = \frac{C}{4 \cdot C_{TH} \cdot R_{TH} \cdot P} \cdot \left(u^2 + u \cdot \sqrt{u^2 - 4 \cdot P \cdot R}\right) - \frac{1}{2} \cdot \frac{\tau}{\tau_{TH}}, \quad (52)$$

$$m_0 = \frac{C}{4 \cdot C_{TH} \cdot R_{TH} \cdot P} \cdot \left(u_0^2 + u_0 \cdot \sqrt{u_0^2 - 4 \cdot \mathrm{P} \cdot \mathrm{R}}\right) - \frac{1}{2} \cdot \frac{\tau}{\tau_{TH}}, \quad (53)$$

where τ is the electrical time constant, i.e. $R \cdot C$.

From (27), $g^2(i)$ can be calculated as

$$g^2(i) = \frac{P^2}{i^2}. \quad (54)$$

Therefore, the relationship between the temperature and the current can be easily obtained by relating equations (45) and (54).

$$T(i) = T_{amb} + (T_0 - T_{amb}) \cdot exp\left(\frac{k_d}{i^2} - k_a\right) + \frac{b}{2} \cdot exp\left(\frac{k_d}{i^2}\right) \cdot \left(Ei\left(-\frac{k_d}{i^2}\right) - Ei(-k_a)\right). \quad (55)$$

Constants k_d can be calculated as

$$k_d = \frac{P \cdot C}{2 \cdot C_{TH} \cdot R_{TH}}. \quad (56)$$

Electrical power can be expressed as the product of the external voltage and the current,

$$P = u_{C0} \cdot i. \quad (57)$$

By combining (54) and (57), the relationship between the external voltage and g can be obtained as

$$u_{C0} = g. \quad (58)$$

According to (58), the relationship between the temperature and the external voltage is identical to that between the temperature and g given by (45).

$$T(u_{co}) = T_{amb} + (T_0 - T_{amb}) \cdot exp\left(\frac{a \cdot u_{co}^2}{2} - k_a\right) + \frac{b}{2} \cdot exp\left(\frac{a \cdot u_{co}^2}{2}\right) \cdot \left(Ei\left(-\frac{a \cdot u_{co}^2}{2}\right) - Ei(-k_a)\right). \quad (59)$$

All the obtained equations can also be applied to a constant-power charge process just by inverting the power sign. The accuracy of these simple proposed equations is assessed in Section 5 by comparing their results to those obtained when calculating the temperature by using numerical methods to solve differential equation (34).

5. Results and discussion

In this section, the accuracy of all equations proposed is checked by means of two SCs case studies: a) Single constant-power discharge process, and b) a series of constant-power charge/discharge processes.

5.1. Single constant-power discharge

A SCs bank discharge process starting from a 135-V initial voltage and at a 2800-W constant power value during 140 s is studied in this section. The thermal and electrical parameters used in this case study are those in Table 2.

The evolution of the temperature as a function of different variables is obtained by using both numerical methods and the equations proposed in Section 4. The differential equations system to be solved by using numerical methods is

Table 2
Electrical and thermal parameters of the SCS bank.

u_0 (V)	P(W)	C (F)	R (Ω)	C_{TH} (J/°C)	R_{TH} (°C/W)	T_0 (°C)	T_{amb} (°C)
135	2800	60	0.02	10	2	20	20

$$\begin{cases} C\cdot\left(P - R\cdot i^2\right)\cdot i' - i^3 = 0 \\ C_{TH}\cdot T' + \dfrac{T - T_{amb}}{R_{TH}} - R\cdot i^2 = 0 \\ u' + \dfrac{i}{C} = 0 \\ W_{losses}{}' - R\cdot i^2 = 0. \end{cases} \quad (60)$$

which is solved by using a 3rd-order Runge-Kutta method with a 1-μs step size. Figs. 7–10 show the evolution of the temperature of the SC as a function of, respectively, time, the internal voltage, the current and the external voltage when solving (60) by using numerical methods (blue plot) or by using (red dots) equations (46)–(49) for Fig. 7, (51)–(53) for Fig. 8, (55) for Fig. 9, and (59) for Fig. 10. Notice that the values of the current in Fig. 9 are negative because they correspond to a discharge process. As can be seen, the accuracy of all equations proposed in Section 4 is remarkable.

5.2. Succession of charge/discharge processes at constant power

In this section, a series of constant-power charge/discharge processes applied to a SCs bank is studied. Results regarding the internal voltage, the current, the temperature, etc., are obtained by using both numerical methods and the equations proposed in sections 3 and 4. The thermal and electrical parameters used in this

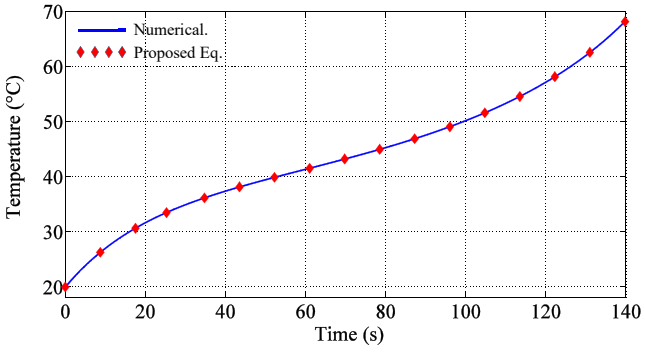

Fig. 7. Temperature as a function of time when using numerical methods (blue plot), and equations (46)–(49) (red dots). (For interpretation of the references to colour in this figure legend, the reader is referred to the Web version of this article.)

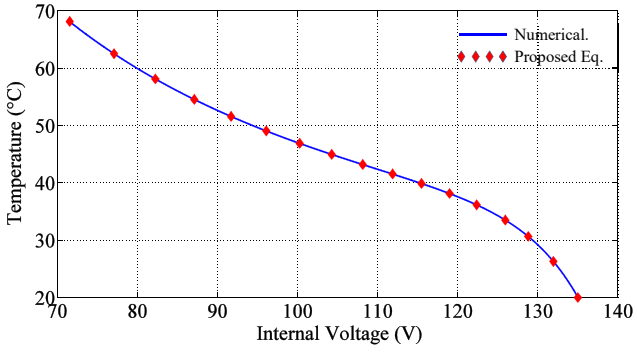

Fig. 8. Temperature as a function of the internal voltage when using numerical methods (blue plot), and equations (51)-(53) (red dots). (For interpretation of the references to colour in this figure legend, the reader is referred to the Web version of this article.)

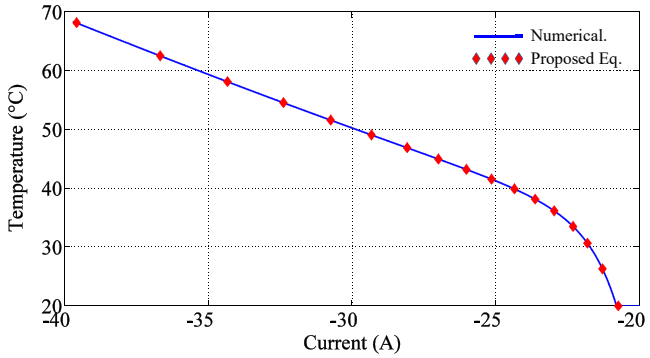

Fig. 9. Temperature as a function of the current when using numerical methods (blue plot), and equation (55) (red dots). (For interpretation of the references to colour in this figure legend, the reader is referred to the Web version of this article.)

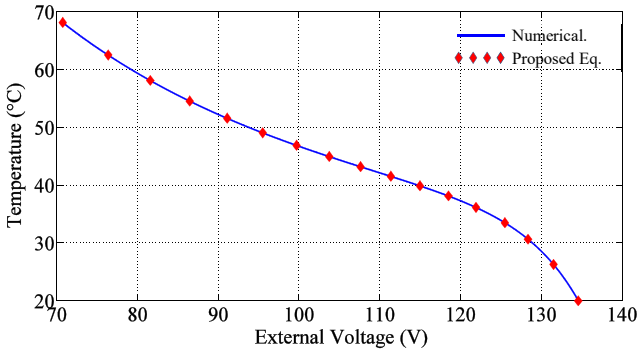

Fig. 10. Temperature as a function of the external voltage when using numerical methods (blue plot), and equation (59) (red dots). (For interpretation of the references to colour in this figure legend, the reader is referred to the Web version of this article.)

case study are those in Table 2. The duration of the simulation is 600 s to ensure that the thermal steady-state is reached, while both the charge and the discharge processes both last 100 s. The initial internal voltage is 135 V. The constant power value for the discharge processes is set at 2000 W, whereas that for the charge processes is set at 2019.27 W to compensate for the internal resistance losses and for the initial internal voltage to keep its value at each cycle. These data are shown in Table 3.

Figs. 11–15 show the evolution over time of, respectively, the internal voltage, the external voltage, the current, the power losses at the internal resistance, and the dissipated heat energy at the cell, by using numerical methods (blue plot) or by using (red dots) equations (21)-(22) for Fig. 11, (22) and (58) for Fig. 12, (28) for Fig. 13, (22) and (29) for Fig. 14, and (32) for Fig. 15.

As explained in Section 4 and seen in Fig. 12, the external voltage values and the results yielded by function $g(t)$ are remarkably similar to each other, which allows for the estimation of the cell temperature simply by measuring the external voltage and assuming that its thermal and electrical parameters are known.

Fig. 16 shows the evolution of the SCs bank temperature by using numerical methods (blue plot) and by using equations (46)–(49) (red dots). The ambient temperature (i.e. the initial temperature of the SCs bank) is set to 20 °C to better observe the thermal transient behaviour.

Fig. 17 shows both a detail of Fig. 16 once the thermal steady-state has been reached and the evolution of the corresponding power losses.

As can be seen, there is a delay between the variables shown in Fig. 17, i.e. the maximum temperature at each cycle is reached some

Table 3
Parameters of the charge and discharge processes.

Charge				Discharge			
u_{min}(V)	u_{max}(V)	P(W)	t(s)	u_{min}(V)	u_{max}(V)	P(W)	t (s)
107.4	135	2019.27	100	107.4	135	2000	100

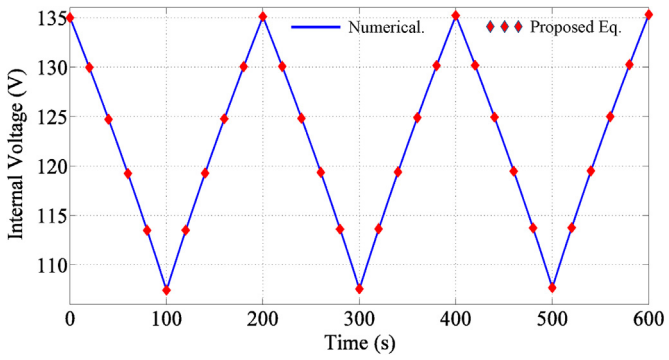

Fig. 11. Internal voltage when using numerical methods (blue plot), and equations (21) and (22) (red dots). (For interpretation of the references to colour in this figure legend, the reader is referred to the Web version of this article.)

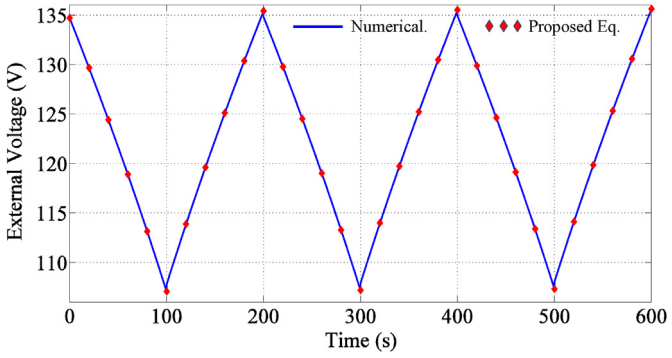

Fig. 12. External voltage when using numerical methods (blue plot), and equations (22) and (58) (red dots). (For interpretation of the references to colour in this figure legend, the reader is referred to the Web version of this article.)

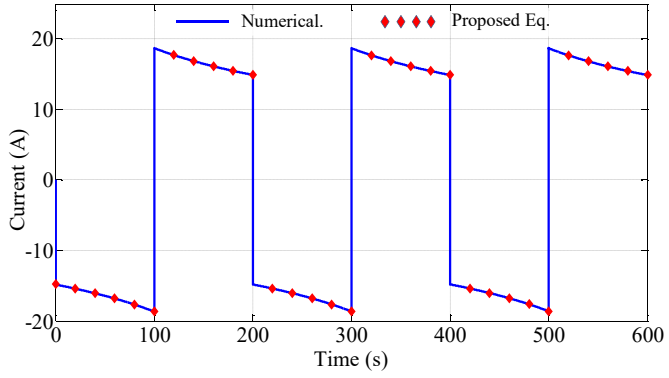

Fig. 13. Current when using numerical methods (blue plot), and equation (28) (red dots). (For interpretation of the references to colour in this figure legend, the reader is referred to the Web version of this article.)

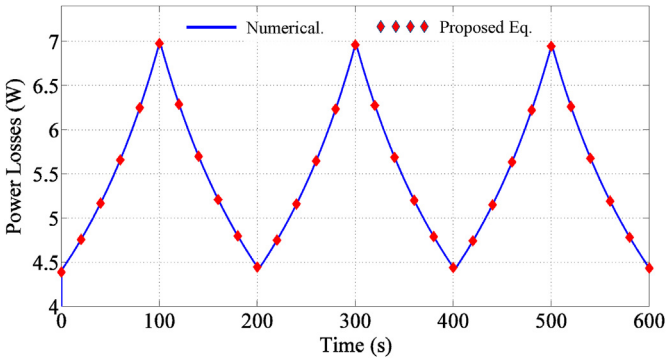

Fig. 14. Power losses at the internal resistance when using numerical methods (blue plot), and equations (22) and (29) (red dots). (For interpretation of the references to colour in this figure legend, the reader is referred to the Web version of this article.)

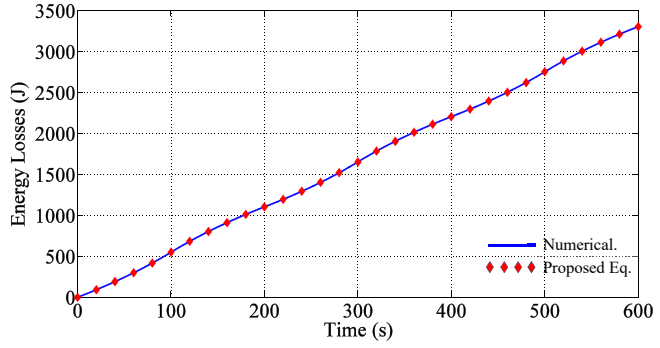

Fig. 15. Dissipated heat energy when using numerical methods (blue plot), and equation (32) (red dots). (For interpretation of the references to colour in this figure legend, the reader is referred to the Web version of this article.)

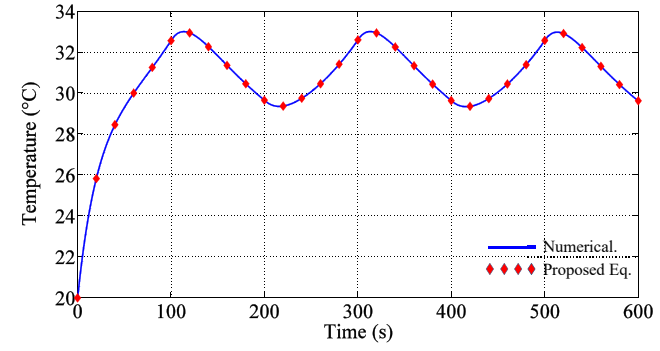

Fig. 16. Temperature when using numerical methods (blue plot), and equations (46)–(49) (red dots). (For interpretation of the references to colour in this figure legend, the reader is referred to the Web version of this article.)

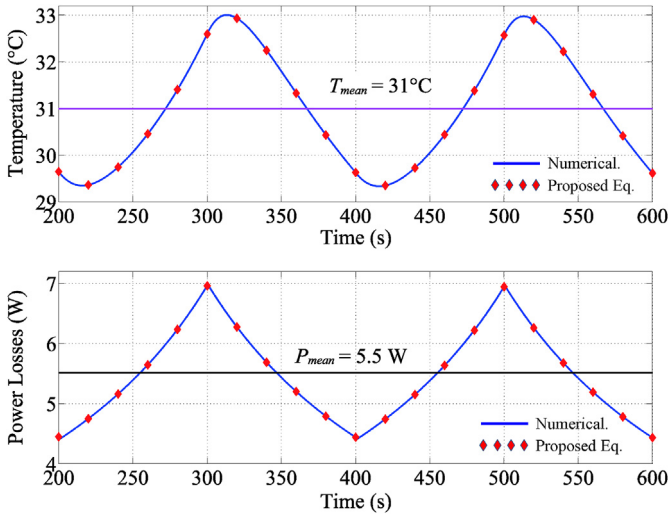

Fig. 17. Top plot: Temperature vs time when using numerical methods (blue plot), and equations (46) – (49) (red dots). Bottom plot: Power losses vs time when using numerical methods (blue plot), and equations (22) and (29) (red dots). (For interpretation of the references to colour in this figure legend, the reader is referred to the Web version of this article.)

time after the maximum power is lost. This delay is related to the thermal constant time, τ_{th}; the higher its value, the longer the delay. Fig. 17 also shows the cell mean temperature, T_{mean}, which can be obtained from the mean value of the power losses, 5.5 W, the ambient temperature, 20 °C, and the thermal resistance,

$$T_{mean} = T_{amb} + R_{TH} \cdot (P_{losses})_{mean} = 31°C. \quad (61)$$

The relationship between the temperature and the internal voltage, the current or the external voltage can also be obtained as done for case study I. For instance, Fig. 18 shows the relation between the temperature and the internal voltage taking only the values at the thermal steady-state for the sake of clarity, both by using numerical methods (blue plot) and equations (51) and (53) (red dots).

Table 4 shows the values of all studied variables when the error is the maximum, obtained both by numerical methods and by using the equations proposed in sections 3 and 4. As seen in Table 4, the proposed approximations yield values remarkably similar to those obtained when utilizing numerical methods.

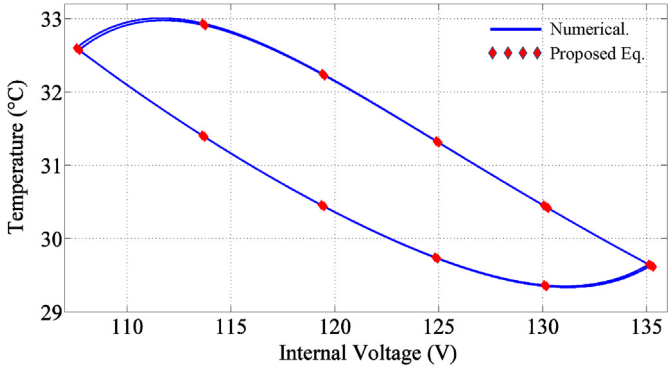

Fig. 18. Temperature as a function of the internal voltage when using numerical methods (blue plot), and equations (51)-(53) (red dots). (For interpretation of the references to colour in this figure legend, the reader is referred to the Web version of this article.)

Table 4
Accuracy of proposed equations.

Variable	Numerical methods	Proposed equations	Absolute error	Relative error (%)
External voltage (V)	135.6022	135.6144	0.0122	0.009
Internal voltage (V)	135.3041	135.3165	0.0121	0.0089
Current (A)	14.8911	14.8897	0.0014	0.0094
Power losses (W)	4.43492	4.43411	0.00081	0.018
Energy losses (J)	3305.187	3304.74	0.4476	0.0135
Temperature (°C)	29.6191	29.6178	0.001238	0.0042

6. Conclusion

A novel analytical approach to calculate the time evolution of the temperature of SC banks operating at constant-power charge/discharge processes has been proposed in this paper. The obtained equations are noticeable simple, accurate and their use is straightforward. Equations regarding temperature as a function of other variables such as the internal voltage, the external voltage or the current are also obtained. Only the thermal and electrical parameters of the cell are needed to solve the proposed equations. Those parameters are usually provided by the manufacturer or can be easily calculated by means of simple experimental tests. Moreover, new remarkably accurate equations to obtain the evolution of the current, the power losses or the dissipated energy have also been proposed. All the proposed equations have proven to be remarkably accurate and yield results noticeable similar to those obtained by using numerical methods. Therefore, the approach proposed in this paper proves to be a reliable and useful means to design the refrigeration system in SCs banks.

Acknowledgements

This work has been funded by the Spanish Government, Innovation Development and Research Office (MEC), under research grants DPI2017-83804-R, and DPI2017-89186-R.

References

[1] Miller J. Introduction to electrochemical capacitor technology. IEEE Electr Insul Mag Jul. 2010;26(4):40–7.
[2] Somayajula D, Crow ML. An integrated dynamic voltage restorer-ultracapacitor design for improving power quality of the distribution grid. IEEE Trans. Sustain. Energy Apr. 2015;6(2):616–24.
[3] de la Torre S, Sánchez-Racero AJ, Aguado JA, Reyes M, Martínez O. Optimal sizing of energy storage for regenerative braking in electric railway systems. IEEE Trans Power Syst May 2015;30(3):1492–500.
[4] Kim Y, Raghunathan V, Raghunathan A. Design and management of battery-supercapacitor hybrid electrical energy storage systems for regulation services. IEEE Trans Multi-Scale Comput Syst Jan.-Mar. 2017;3(1):12–24.
[5] Song Z, Hou J, Hofmann H, Li J, Ouyang M. Sliding-mode and Lyapunov function-based control for battery/supercapacitor hybrid energy storage system used in electric vehicles. Energy Mar. 2017;122(1):601–17.
[6] Kouchachvili L, Yaïci W, Entchev E. Hybrid battery/supercapacitor energy storage system for the electric vehicles. J Power Sources Jan. 2018;374(15):237–48.
[7] Luta DN, Raji AK. Optimal sizing of hybrid fuel cell-supercapacitor storage system for off-grid renewable applications. Energy Jan. 2019;166(1):530–40.
[8] Duan J, Liu J, Xiao Q, Fan S, Sun L, Wang G. Cooperative controls of micro gas turbine and super capacitor hybrid power generation system for pulsed power load. Energy Feb. 2019;169(15):1242–58.
[9] Li T, Huang L, Liu H. Energy management and economic analysis for a fuel cell supercapacitor excavator. Energy Apr. 2019;172(1):840–51.
[10] Michel Hartmut. Temperature and dynamics problems of ultracapacitors in stationary and mobile applications. J Power Sources February 2006;154:556–60.
[11] Zhang Lei, Hu Xiaosong, Wang Zhenpo, Sun Fengchung, David G. Dorrell "A review of supercapacitor modeling, estimation, and applications: a control/management perspective". Renew Sustain Energy Rev May 2017;81:1868–78.
[12] Gualous H, Gallay R, Alcicek G, Tala-Ighil B, Oukaour A, Boudart B, Makany Ph. Supercapacitor ageing at constant temperature and constant voltage and thermal shock. Microelectron Reliab Aug. 2010;50:1783–8.

[13] Miller JR, Butler S. "Capacitor system life reduction caused by cell temperature variation", 2006 advanced capacitor world summit. 2006. San Diego.
[14] Bohlen O, Kowal J, Sauer DU. Ageing behaviour of electrochemical double layer capacitors Part I. Experimental study and ageing model. J Power Sources 2007;172.
[15] Bohlen O, Kowal J, Sauer DU. Ageing behaviour of electrochemical double layer capacitors Part II. Lifetime simulation model for dynalic applications. J Power Sources 2007;173.
[16] Maxwell technologies: « Application note, life duration estimation». http://www.maxwell.com.
[17] Murray Donal B, Hayes John G. Cycle testing of supercapacitors for long-life robust applications. IEEE Trans Power Electron May 2015;30(5).
[18] Monzer Al Sakka, Gualous Hamid, Van Mierlo Joeri, Culcu Hasan. Thermal modeling and heat management of supercapacitor modules for vehicle applications. J Power Sources June 2009;194:581–7.
[19] Julia Schiffer, Linzen Dirk, Sauer Dirk Uwe. Heat generation in double layer capacitors. J Power Sources February 2006;160:765–72.
[20] Chiang Chia-Jui, Yang Jing-Long, Cheng Wen-Chin. Dynamic modeling of the electrical and thermal behavior of ultracapacitors. In: 2013 IEEE international conference on control and automation (ICCA); 2013. Hangzhou, China, June 12-14.
[21] Miller John M. Electrical and thermal performance of the carbon-carbon ultracapacitor under constant power conditions. In: IEEE vehicle power and propulsion conference. Maxwell Technologies, Inc.; 2007.
[22] Grbovic PJ. Ultra-capacitors in power conversion systems. IEEE Press Wiley; 2013, ISBN 9781118356265.
[23] Miller JM. Ultracapacitor applications. IET Power and Energy Series 2011;59. 9781849190718.
[24] Gao Q, Zou MY. An analytical solution for two and three dimensional nonlinear Burger's equation. J Appl Mathematical Model Dec 2016;45:255–70.
[25] Gómez-Aguilar JF, Yépez Martínez H, Escobar Jiménez RF, Astorga Zaragoza CM, Reyes Reyes J. Analytical and numerical solutions of electrical circuits described by fractional derivatives. J Appl Mathematical Model June 2016;40:9079–94.
[26] Gusso André, Pimentel Jéssica D. Approximate fully analytical Fourier series solution to the forced and damped Helmholtz-Duffing oscillator. J Appl Mathematical Model May 2018;61:593–603.
[27] Ahmed Basha C, Rahamathunissa G, Sivakumar S, Lee Chang Woo. "*Numerical and analytical solution of an ODE: Strengths and weaknesses of the analytical series solution*". J Appl Mathematical Model July 2011;36:618–25.
[28] Foyouzat MA, Estekanchi HE, Mofid M. *An analytical-numerical solution to assess the dynamic response of viscoelastic plates to a moving mass*". J Appl Mathematical Model July 2017;54:670–96.